Received: 1 July 2020 | Accepted: 28 October 2020

DOI: 10.1111/1365-2656.13386

RESEARCH ARTICLE

Journal of Animal Ecology | BRITISH ECOLOGICAL SOCIETY

Preparatory immunity: Seasonality of mucosal skin defences and *Batrachochytrium* infections in Southern leopard frogs

Emily H. Le Sage[1] | **Brandon C. LaBumbard**[2] | **Laura K. Reinert**[1] | **Brian T. Miller**[3] | **Corinne L. Richards-Zawacki**[4] | **Doug C. Woodhams**[2] | **Louise A. Rollins-Smith**[1,5,6]

[1]Department of Pathology, Microbiology, and Immunology, Vanderbilt University School of Medicine, Nashville, TN, USA; [2]Department of Biology, University of Massachusetts, Boston, MA, USA; [3]Department of Biology, Middle Tennessee State University, Murfreesboro, TN, USA; [4]Department of Biological Sciences, University of Pittsburgh, Pittsburgh, PA, USA; [5]Department of Biological Sciences, Vanderbilt University, Nashville, TN, USA and [6]Department of Pediatrics, Vanderbilt University School of Medicine, Nashville, TN, USA

Correspondence
Emily H. Le Sage
Email: e.h.lesage@gmail.com

Funding information
Division of Integrative Organismal Systems, Grant/Award Number: CAREER 1845634; U.S. Department of Defense

Handling Editor: Jon Bielby

Abstract

1. Accurately predicting the impacts of climate change on wildlife health requires a deeper understanding of seasonal rhythms in host–pathogen interactions. The amphibian pathogen, *Batrachochytrium dendrobatidis* (*Bd*), exhibits seasonality in incidence; however, the role that biological rhythms in host defences play in defining this pattern remains largely unknown.
2. The aim of this study was to examine whether host immune and microbiome defences against *Bd* correspond with infection risk and seasonal fluctuations in temperature and humidity.
3. Over the course of a year, five populations of Southern leopard frogs (*Rana* [*Lithobates*] *sphenocephala*) in Tennessee, United States, were surveyed for host immunity, microbiome and pathogen dynamics. Frogs were swabbed for pathogen load and skin bacterial diversity and stimulated to release stored antimicrobial peptides (AMPs). Secretions were analysed to estimate total hydrophobic peptide concentrations, presence of known AMPs and effectiveness of *Bd* growth inhibition in vitro. The diversity and proportion of bacterial reads with a 99% match to sequences of isolates known to inhibit *Bd* growth in vitro were used as an estimate of predicted anti-*Bd* function of the skin microbiome.
4. *Batrachochytrium dendrobatidis* dynamics followed the expected seasonal fluctuations—peaks in cooler months—which coincided with when host mucosal defences were most potent against *Bd*. Specifically, the concentration and expression of stored AMPs cycled synchronously with *Bd* dynamics. Although microbiome changes followed more linear trends over time, the proportion of bacteria that can function to inhibit *Bd* growth was greatest when risk of *Bd* infection was highest.
5. We interpret the increase in peptide storage in the fall and the shift to a more anti-*Bd* microbiome over winter as a preparatory response for subsequent infection risk during the colder periods when AMP synthesis and bacterial growth is slow and pathogen pressure from this cool-adapted fungus is high. Given that

a decrease in stored AMP concentrations as temperatures warm in spring likely means greater secretion rates, the subsequent decrease in prevalence suggests seasonality of *Bd* in this host may be in part regulated by annual immune rhythms, and dominated by the effects of temperature.

KEYWORDS

amphibian disease, annual cycle, *Batrachochytrium*, disease ecology, seasonal immunity, seasonal microbiome

1 | INTRODUCTION

Both hosts and pathogens must cope with annual changes in environmental conditions. From either perspective, physiological processes and rates may vary throughout the year or resource limitations may require conserving and diverting energy, which drive fluctuations in host defences and pathogen growth (Martinez-Bakker & Helm, 2015). These biological rhythms in host and pathogen traits can cause predictable patterns in epidemiological phenomena, such as annual mortality events (reviewed in Altizer et al., 2006). In many cases, the timing of epidemics coincides with host biological rhythms in reproduction, behaviour or life history that affect host defences or transmission rates (Dopico et al., 2015; Hall et al., 2018); whereas, other seasonal disease systems are highly regulated by pathogen traits such as environmental persistence (Jenkins et al., 2006; Shaman et al., 2010). Because climate change projections include greater pathogen pressures (Harvell et al., 2002) and more variable seasonality (Williams et al., 2015), understanding seasonal drivers of disease dynamics is increasingly relevant for global health (Altizer et al., 2013). Whether hosts and pathogens can adapt to predicted changes in seasonality depends on the mechanisms underlying their biological rhythms (Stevenson et al., 2015).

Annual photoperiod, temperature and precipitation cycles provide predictable cues of seasonal transitions used to entrain biological rhythms (e.g. life cycle events; Visser et al., 2010). Perhaps one of the most researched regulators of seasonal immunity, temperature drives an adaptive reorganization of immune components, cells and tissues in many organisms (reviewed in Nelson & Demas, 1996). Cold temperatures, which can slow enzymatic or cellular activity, can also coincide with times when resources needed for specific immune functions are limited (reviewed in Sandmeier et al., 2016). Temperature can also regulate annual rhythms of life cycles that sometimes involve trade-offs with immunity, potentially regulated by immunomodulatory hormones such as androgens and glucocorticoids (Sheldon & Verhulst, 1996; Szwejser et al., 2017). Seasonal and temperature influences also extend to microbiome diversity and richness (Davenport et al., 2014; Estrada et al., 2019) and these shifts are predicted to play a role in disease dynamics (Longo et al., 2015; Runckel et al., 2011). Not only are hosts, microbes and parasites constrained by their environmental niche, temperature-entrained rhythms can affect other aspects of epidemiology including pathogens' 'temporal niche' (reviewed in Altizer et al., 2006; Grassly & Fraser, 2006; Martinez-Bakker & Helm, 2015). For example, timing of pathogen introduction into the population (e.g. migration), host contact rates (e.g. aggregation) or density of susceptible individuals (e.g. birth rates) can drive seasonal disease incidence. Altogether, accurate model predictions of epidemiological and evolutionary processes regulating seasonal host–pathogen dynamics depend on observations of natural biological rhythms.

Here, we studied the natural course of host–microbiome–pathogen–environment associations in Southern leopard frog populations (*Rana* [*Lithobates*] *sphenocephala*) and the infectious chytrid fungus, *Batrachochytrium dendrobatidis* (*Bd*). The *Bd* pathogen has been linked to population declines of amphibians globally and displays seasonal fluctuations in prevalence, intensity and mortality from infection (e.g. Berger et al., 2004; reviewed in Fisher et al., 2009). Often the seasonal dynamics of *Bd* is attributed to the temperature-dependent growth of the pathogen; however, the relative role of seasonality in host defences remains an open question (reviewed in Rollins-Smith, 2020). Therefore, we hypothesize that the periodic incidence of *Bd* infections is either a consequence of host or microbiome rhythms entrained to seasonal cues (e.g. temperature or time of year) or governed by pathogen traits that operate independently of host or microbiome rhythms. As a barrier defence, the presence and abundance of anti-*Bd* antimicrobial peptides (AMPs) and bacteria in the mucosal epidermal layer have been associated with individual, population and species differences in susceptibility to *Bd* infection (Bletz et al., 2013; Holden, Hanlon, et al., 2015; Voyles et al., 2018; Woodhams et al., 2014). Thus, to assess whether *Bd* dynamics follow cycles in these critical host skin defences, we captured frogs in field surveys and quantified total stored peptide concentrations, *Bd*-inhibitory activity of secretions, AMP presence, microbiome richness and diversity, presence of bacteria corresponding to anti-*Bd* isolates, and *Bd* infections throughout the active season of amphibian hosts.

2 | MATERIALS AND METHODS

2.1 | Ethics statement

This study was approved by Vanderbilt University Medical Center IACUC and the Tennessee Wildlife Resources Agency. Permission was granted from the Arnold Air Force Base to conduct research. Gear was decontaminated between sites using fresh 10% bleach and rinsed with clean water according to best biosecurity practices (Gray et al., 2017).

2.2 | Field surveys

Five sites within the Arnold Engineering Developmental Center wildlife management area near Tullahoma, Tennessee, USA were selected for field surveys (Table S1 for locations; sites were approx. 0.8–10.3 km apart). Using the astronomical definition, surveys spanned all four seasons in 2017, with one visit in winter (March 3–20), three visits in spring (March 22–May 8), four visits in summer (June 27–August 11) and four visits in fall (September 29–November 11) at each of the five sites. Just after sunset, sampling surveys were conducted for 1–2 hr. Here, frogs were captured with gloved hands and held in individual plastic re-sealable bags. Before capture, body temperatures were measured using an infrared thermometer (Etekcity Lasergrip 774; ±2°C accuracy). Gloves were changed and nets were rinsed between individuals to prevent contamination. Each frog was weighed to the nearest 0.1 gram using a Pesola scale; snout–vent length (SVL) was measured using digital callipers; and life stage and sex were recorded. At each site, temperature and relative humidity were logged at 30 min intervals at 0.5 m above the leaf litter in the shade near the wetland edge (HOBO, Onset). After processing, frogs were released near the location of capture.

2.3 | Pathogen diagnostics

Animals were swabbed for *Bd* and *Bsal* (*B. salamandrivorans*) presence and infection intensity by stroking each foot and body surface (dorsal, ventral and each side) five times with a cotton swab (Hyatt et al., 2007). Swabs were frozen, then processed for *Bd* and *Bsal* at the University of Pittsburgh. Genomic DNA was extracted using the Qiagen DNeasy Blood and Tissue Kit according to the manufacturer's protocol for animal tissue with the following modifications: swabs were incubated for 30 min, vortexed and spun in a centrifuge, and then incubated for another 30 min. Samples were eluted two times with 100 μl of elution buffer for a final elution volume of 200 μl. The duplex qPCR assay followed Blooi et al. (2013), except that it also included an internal positive control (Hyatt et al., 2007) and bovine serum albumin (final concentration 400 ng/μl; Garland et al., 2010) in each reaction well. Positive and negative controls and a sevenfold dilution series of plasmid-based *Bd* and *Bsal* standards (Pisces Molecular, Boulder CO) were included in each qPCR run. Each swab extract was tested once (singlicate) to maximize cost efficiency (Kriger et al., 2006). *Bd* load per 5 μl reaction volume was converted to whole-swab loads, and these values were $\log_{10}$-transformed before analysis.

2.4 | Peptide recovery

After swabbing, frogs were placed for a 1-hr soak in sterile water to collect washes for a separate study. After this soak, frogs were stimulated to release peptides with an injection of 40 nmol/g body weight norepinephrine bitartrate (Rollins-Smith, Doersam, et al., 2002). Peptide secretions were collected in 50 ml of HPLC-grade water for 15 min. From this sample, a 25 ml subsample was acidified (concentrated HCl added to achieve 1% v/v) then frozen. Note that this approach yields amounts representing the quantity stored in the granular glands, not the rate of synthesis or constitutive concentrations in the skin mucus, and this dose does not deplete granular glands but is likely more stimulatory than a predator encounter (Ramsey et al., 2010). To enrich for hydrophobic compounds, secretions were passed over C-18 Sep-Pak cartridges (Waters Corporation), eluted with 70% acetonitrile, 29.9% water and 0.1% trifluoroacetic acid and dried under vacuum at 70°C. Peptide concentrations were quantified by averaging triplicate wells in a micro BCA (Thermo Fisher Scientific) assay using bradykinin diluted in the elution buffer as a standard (six dilutions) after the blank (elution buffer) was subtracted. Samples were re-run if the coefficient of variation was >15% among triplicates. Recovered peptide concentrations were correlated with body weight ($p < 0.001$) but not body condition (scaled mass index: $p = 0.236$), therefore the amount of peptides in each mL of mucus was estimated using the method in Pask et al. (2012). This method assumes a mucus thickness of 50 μm, and therefore 5 μl of mucus covers 1 cm^2. The concentration of peptides in μg/ml in mucus is equal to total peptides (μg) divided by body surface area $[9.9 \times (\text{body weight})^{0.56}] \times 200$. Matrix assisted laser desorption time of flight (MALDI-TOF) mass spectrometry was used to determine the presence and relative intensity of the four previously described AMPs found in Southern leopard frog enriched secretions reconstituted in HPLC-grade water at 1 mg/ml (Conlon et al., 1999; Holden, Reinert, et al., 2015). Individuals were photographed and compared side by side and identified using their unique spot patterns, which maintain relative positions in adults. Recaptures caught within 2 weeks were removed from analysis of AMPs because animals are still recovering reserves within that timeframe.

2.5 | Growth inhibition assays

In a subset of samples, the effectiveness of recovered peptides at inhibiting *Bd* growth in culture was quantified by following methods of Rollins-Smith, Doersam, et al. (2002). *Bd* isolate JEL-197 (the original type strain; in the global panzootic lineage) zoospores in 1% tryptone broth (5×10^4 μl^{-1}) were plated with serial dilutions of filter sterilized peptides in sterile HPLC-grade water for 7 days at 22°C. Three to five replicates were plated at twofold dilutions from 500 to 15.6 μg/ml. The minimum inhibitory concentration (MIC) was defined as the lowest concentration at which growth was not detectable. Percent inhibition at 125 μg/ml was calculated as the per cent growth of the positive control (zoospores plated without peptides). MIC equivalents (calculated by dividing total recovered peptides by the MIC) in mucus, or per cent inhibition at 125 μg/ml recovered peptides, were tested for differences among seasons using a Kruskal–Wallis test (winter and spring samples were combined in this analysis; $N = 8$–17/season).

2.6 | Microbiome analysis

Two of the five sites were chosen for microbiome analysis and sample sizes for each survey are in Table S2. Frogs were swabbed

twice on the same surfaces as the *Bd* swab after the sterile water bath and before stimulating peptide release. Swabs were frozen at −80°C until processing. DNA was extracted using a DNeasy Blood & Tissue Kit (Qiagen, Inc.) following the manufacturer's protocol with the following modifications. An initial lysozyme (20 mg lysozyme/mL lysis buffer) incubation step at 37°C for 1 hr was included to help lyse gram-positive bacteria, and then 25 μl proteinase K was added to each reaction in addition to 200 μl buffer AL (DNeasy kit lysis buffer), and incubated at 70°C for 30 min. PCR was conducted to amplify the V4 region of the 16 rRNA gene (515F and 806R primers) following the Earth Microbiome protocol methods of (Caporaso et al., 2012) except that PCR reactions were run in duplicate instead of triplicate. Amplicons from duplicate reactions were pooled and visualized on 1.5% agarose gels and then purified and normalized using a Mag-Bind EquiPure Library Normalization Kit (Omega Biotek, Inc.). After normalizing, all samples were pooled for library preparation and the library was sequenced at the University of Massachusetts Boston Biology Department using an Illumina MiSeq v2 300 cycles cartridge.

The raw Illumina 16S rRNA amplicon data were quality filtered using QIIME2 2019.10 (Bolyen et al., 2018) and classified into sub-operational taxonomic units (sOTUs) using the Deblur workflow (Amir et al., 2017). Within Deblur, reads were trimmed to 150 bp and bacterial taxonomy was assigned using the Greengenes 13_8 99% OTUs reference classifier (McDonald et al., 2012). The sOTUs assigned as 'mitochondria' and 'chloroplast', as well as reads found in negative controls (field control swabs rinsed with sterile water used for frogs and extraction control swabs) were deemed as contaminants and were filtered out. The dataset was rarefied at 1,200 sequences per sample to retain most samples and to normalize read counts across samples. Several core metrics were generated for exploring differences in alpha diversity (sOTU richness and Faith phylogenetic distance) and beta diversity (Bray–Curtis, Jaccard, Unweighted and Weighted UniFrac). Community structure and bipartite networks were calculated in R (Sedlar et al., 2016) and visualized using *Gephi* (Bastian et al., 2009) to show the association of bacterial taxa across seasons. The core microbiome found in 80% of samples was calculated in QIIME2. A differential abundance analysis was performed using Aldex2 (Fernandes et al., 2014) to look for microbial differences between infection status and among seasons. The correlation between the Bray–Curtis distance matrix of bacterial sOTUs and the Bray–Curtis distance matrix of peptide peaks (larger than 5% relative intensity) was analysed using a mantel test (VEGAN package Oksanen et al., 2019) and visualized by Procrustes analysis in QIIME2.

To determine predicted anti-*Bd* function, sequences were compared to the Antifungal Isolates Database (Woodhams et al., 2015) using the vsearch cluster-features-closed-reference script (Rognes et al., 2016) to identify sequences with 99% match to bacterial isolates previously shown to inhibit *Bd* growth in culture by at least 80% compared to controls. This estimation of microbial community function comes with uncertainty, but may be useful for between-group comparisons (Langille et al., 2013), and we note that the function of microbial secondary metabolites can differ among *Bd* isolates (Antwis & Harrison, 2018), and that 16S rRNA sequences may not faithfully indicate secondary metabolite production, although function can be a phylogenetically conserved trait (Goelen et al., 2020).

2.7 | Laboratory overwintered Northern leopard frogs

To examine whether overwintering affects AMP synthesis, adult Northern leopard frogs (*Rana* [*Lithobates*] *pipiens*; $N = 10$) were obtained from Minnesota (BioCorporation, Alexandria, MN) in the fall of 2004. This experiment with a closely related species fills an important gap in our understanding of recovery near freezing temperatures, as previous work is restricted to >14°C and we were unable to survey wild overwintering animals for AMP recovery. All were induced to secrete peptides with 40 nmol/g norepinephrine bitartrate as described above and similar peptide profiles and concentrations were recovered ($p = 0.99$). Four frogs were then placed in 4°C and six frogs were kept at room temperature (~21°C) for 5 weeks (February–March) until they were induced for peptides again by injection with 10 nmol/g norepinephrine bitartrate at day 35. These samples were analysed for peptide concentration and effectiveness at inhibiting *Bd* growth using the aforementioned methods. Peptide effectiveness was calculated by multiplying peptide concentration (μg/g body mass) by per cent *Bd* growth inhibition at a 50 μg/ml peptide concentration. Variation in peptide effectiveness among frogs held at 4 and 21°C was tested with nonparametric statistics due to data distribution.

2.8 | Statistical analyses

Statistical analyses were performed in R v. 3.6.1. Generalized additive models across survey dates were used to explore the temporal dynamics of temperature, *Bd* prevalence and load (copies), recovered peptides, bacterial sOTU richness, and the proportion of the microbiome that corresponds to anti-*Bd* bacteria. Because temperature was correlated with several mucosal attributes, the method of Raffel et al. (2006) was used to isolate the effect of season after accounting for temperature. Specifically, the residuals of a linear model of host traits by average daily air temperature with site as a covariate was analysed as the dependent variable in an ANOVA (or Kruskal–Wallis test when the assumption of normality was not met) with season as the independent variable. If temperature was not an important predictor of host traits, these residuals were not used in place of the raw data. Relationships among seasons and infection status and diversity indices of either peptide or microbiome profiles were analysed using PERMANOVAs with site included as strata (*adonis2* in VEGAN package). Univariate mixed models were used to explore relationships between each mucosal attribute and with *Bd* infection (logistic; *glmer*) or load (linear; *lmer*) with site as a random variable (LMERTEST package Kuznetsova et al., 2017). Only two females and one juvenile

were captured in winter and spring sampling events, thus sex and life stage differences are compounded with seasonal effects.

3 | RESULTS

3.1 | Host–microbiome–pathogen temporal dynamics

In 2017, 168 Southern leopard frogs were swabbed during 35 of the 60 survey visits that spanned all four seasons (see Table S2 for sample sizes). Eight frogs were recaptured at least once and one was recaptured twice, for a total of 178 swabs for *Bd* diagnostics from five sites and 84 swabs for microbiome analysis from two sites. In general, the seasonal dynamics of *Bd* infection inversely followed temperature changes. That is, as temperatures rose from March through August, *Bd* prevalence gradually decreased to the lowest levels in August. As temperatures cooled in October and November, *Bd* prevalence and infection intensity (positives only) increased (Figure 1a–c). Mirroring *Bd* dynamics, AMPs also inversely followed temperature changes. Concentrations of recovered peptides (per mL of mucus) were greatest in March through May, declined during the warmer months, and then increased in the fall (Figure 1d). Unlike *Bd* and peptide dynamics, bacterial sOTU richness had a more linear relationship over time (Figure 1e). Predicted anti-*Bd* function (sequence read abundance) decreased as the year progressed from March to November (Figure 1f), while predicted anti-*Bd* sOTU richness increased over time.

3.2 | Batrachochytrium prevalence and burden

Bsal was not detected in any of the swab samples. The prevalence of *Bd* infection varied by site ($\chi^2 = 18.207$, $df = 4$, $p = 0.001$), but overall was 49% from March to May ($N = 53$), then dropped to 18.5% in the summer ($N = 54$), and rose again to 37% in the fall ($N = 70$). Daily average air temperature and relative humidity were negatively related to the probability of infection (GLMM with site as a random variable; $N = 176$; $\beta_{\text{Temperature}} = -0.092 \pm 0.038$, $z = -2.411$, $p = 0.016$; $\beta_{\text{Humidity}} = -0.02 \pm 0.011$, $z = -1.975$, $p = 0.048$). Body temperature at the time of capture showed only a weak relationship to probability of infection ($N = 144$; $\beta_{\text{Temperature}} = -0.092 \pm 0.049$, $z = -1.902$, $p = 0.057$). After accounting for the effects of temperature (by comparing residuals), the probability of infection did not vary by season ($p = 0.40$).

In contrast with prevalence, *Bd* loads of infected frogs were not correlated with temperature (maximum/average air temperature or body temperature $p < 0.05$) or humidity ($p = 0.27$). However, there was a seasonal effect on *Bd* loads (LMM; Season: $\chi^2 = 8.948$, $p = 0.03$). Specifically, *Bd* loads of infected frogs were on average 12 times higher in winter (17,010 ± 8,403 copies) compared to summer (1,397 ± 631 copies).

3.3 | Mucosal peptide concentrations and AMP expression

After accounting for temperature and site effects, recovered hydrophobic peptide concentrations varied by season (Kruskal–Wallis,

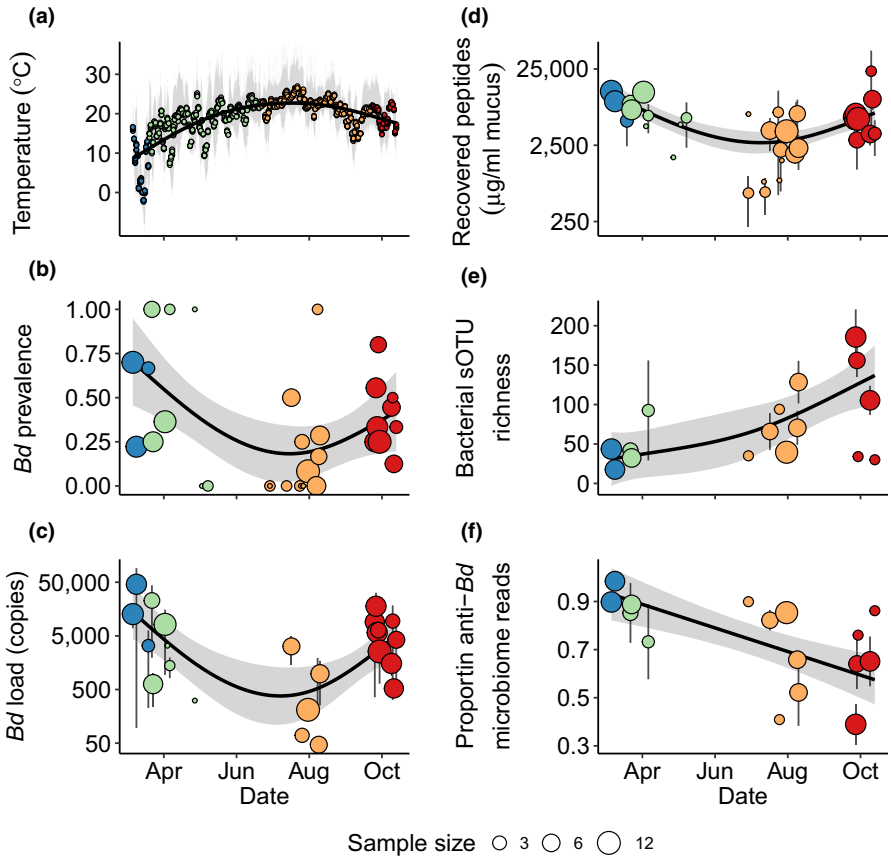

FIGURE 1 Temporal changes in temperature, *Batrachochytrium dendrobatidis* (*Bd*) dynamics and Southern leopard frog mucosal defences. (a) Daily average air temperature from temperature loggers at the five sites. (b) *Bd* prevalence in Southern leopard frogs (proportion infected of total sampled). (c) Average (±*SEM*) *Bd* load of infected animals (qPCR positives only). (d) Average (±*SEM*) recovered peptide levels (µg/ml mucus by surface area). (e) Average (±*SEM*) bacterial sOTU richness (operational taxonomic units) from skin swabs. (f) Average (±*SEM*) predicted anti-*Bd* function of the microbiome (proportion of bacterial reads known to inhibit *Bd* in vitro of the total microbiome reads). All points are sized by sample size ($N = 1$–12 per survey) according the legend at the bottom of the figure and coloured according to season. Lines and shading represent generalized additive models and 95% confidence intervals

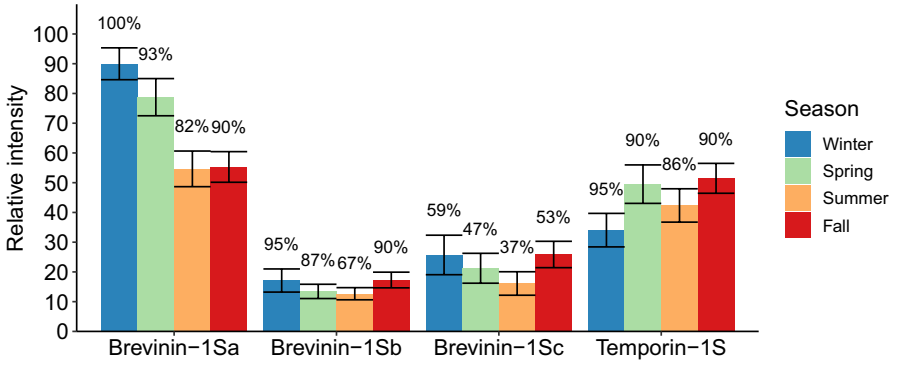

FIGURE 2 Seasonal dynamics of identified antimicrobial peptides in Southern leopard frog mucus. Bars (coloured to represent each season) depict the average (±*SEM*) relative intensity of antimicrobial peptides (AMPs) in MALDI-TOF spectra with the percent of frogs found expressing AMPs above each bar (sample sizes: winter = 22, spring = 30, summer = 51, fall = 58)

$\chi^2 = 8.642$, $p = 0.034$). Specifically, summer frogs exhibited lower concentrations for a given temperature compared to winter. At the individual level, recovered peptide concentrations did not predict the probability of infection ($p = 0.330$); however, there was a significant interaction between season and peptide concentration on the intensity of infections (Interaction: $\chi^2 = 8.843$, $p = 0.032$), in that only in winter frogs with lower peptide concentrations also had lower *Bd* loads. At the population level, the average peptide concentration was positively related to the average *Bd* load at each survey (positives only; $\beta_{\text{Avg peptide}} = 1.335 \pm 0.545$, $t_{22} = 2.448$, $p = 0.023$).

When analysed by mass spectrometry, most frogs (141/161) expressed at least three of the four previously described AMPs for this species (temporin-1S, m/z 1,444; brevinin-1Sa, m/z 2,521; brevinin-1Sb, m/z/ 2,537; and brevinin-1Sc, m/z 2,612; Conlon et al., 1999; Holden, Hanlon, et al., 2015). However, whether frogs were observed expressing each AMP varied by season (Figure 2). Specifically, fewer summer frogs were expressing brevinin-1Sa and -1Sb ($\chi^2 = 4.892$, $p = 0.03$; $\chi^2 = 6.857$, $p = 0.009$), and slightly fewer expressed -1Sc ($\chi^2 = 2.977$, $p = 0.08$) than winter frogs. Furthermore, lower relative intensities of brevinin-1Sa were observed in summer compared to winter (GLMER; $z = -2.639$, $p = 0.038$). Frogs also expressed different patterns of the presence/absence and relative intensity of all peptide molecular species in MALDI-TOF spectra (Jaccard's index: $F = 2.115$, $p = 0.001$; Bray–Curtis index: $F = 2.532$, $p = 0.002$; Figure 3a,b). However, peptide composition did not vary by infection status (Jaccard's index: $p = 0.585$; Bray–Curtis index: $p = 0.375$).

Among seasons, the minimal inhibitory concentration (MIC) for peptide mixtures did not differ in *Bd* growth inhibition assays (Kruskal–Wallis test; $p = 0.76$), nor did samples differ in percent inhibition at 125 μg/ml (Logistic regression; $p = 0.75$) or MIC equivalents per mL of mucus (ANOVA; $p = 0.61$).

3.4 | Diversity of skin bacteria

Bacterial richness gradually increased from March through November. Specifically, skin swabs had on average 29 ± 5 sOTUs in winter and rose to 140 ± 17 sOTUs by fall. After accounting for temperature, seasonal differences in total bacterial richness (sOTUs) and the predicted anti-*Bd* function were significant (sOTUs: ANOVA; $F = 13.54$, $p < 0.001$; proportion anti-*Bd*: Kruskal–Wallis; $\chi^2 = 16.142$, $p = 0.001$). Neither

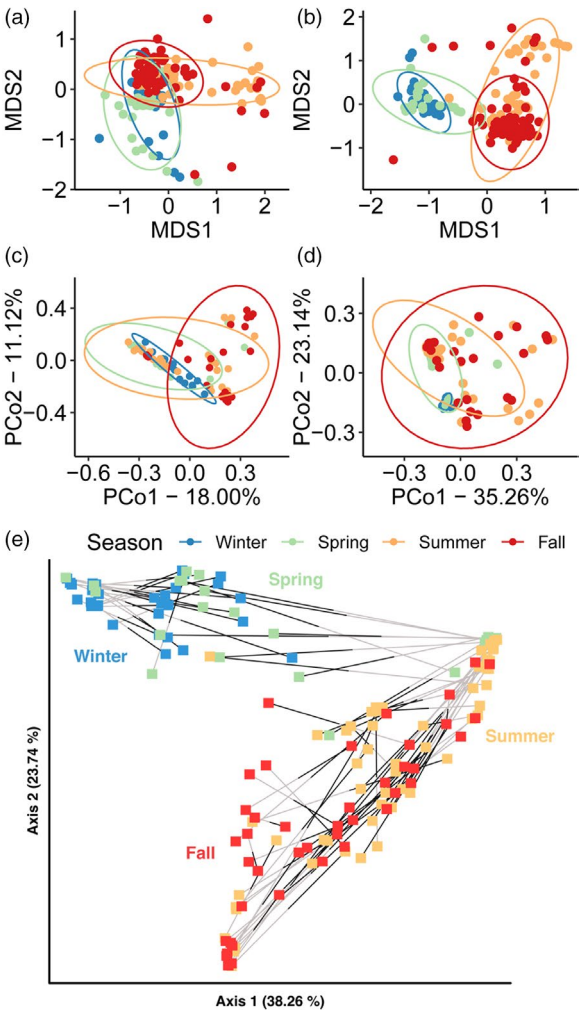

FIGURE 3 Patterns of peptide (a, b) and microbiome (c, d) profiles depended on season and the pairwise distances were related to one another. Multidimensional scaling of (a) presence/absence, and the (b) the area of mass spectral peaks from MALDI-TOF of enriched peptide samples which included peaks with >5% relative intensity binned to 1 m/z, and if there were multiple peaks within 1 m/z, only the area of the first peak was used ($N = 152$). Principal coordinate analyses of microbiome beta diversity using (c) Unweighted UniFrac index and (d) Weighted UniFrac index ($N = 84$). (e) Procrustes plot of the correlation between the Bray–Curtis distance matrix in bacterial sOTUs (point connected to gray line) and the Bray–Curtis distance matrix in peptide MALDI peaks with >5% relative intensity (point connected to black line; $N = 78$)

the predicted anti-*Bd* function nor the predicted anti-*Bd* bacterial richness predicted *Bd* load (Proportion: $p = 0.398$, sOTUs: $p = 0.957$) or infection status (Proportion: $p = 0.416$, sOTUs: $p = 0.439$). Patterns of beta diversity also displayed clustering by season (Weighted UniFrac index: $F = 6.737$, $p = 0.001$; Jaccard's index: $F = 3.436$, $p = 0.001$; Bray–Curtis index: $F = 12.307$, $p = 0.001$; Figure 3c,d). Similar to peptide profiles, skin bacterial beta diversity was unrelated to *Bd* infection status (Weighted UniFrac index: $F = 1.549$, $p = 0.184$; Jaccard's index: $F = 1.399$, $p = 0.064$; Bray-Curtis index: $F = 1.583$, $p = 0.151$). Within individuals, the pairwise distances of mucosal defences were positively related, specifically there was a strong correlation between Bray–Curtis distance matrices of each microbiome and peptide profiles (Mantel $r = 0.214$, $p < 0.001$; Figure 3e). Both bacterial and peptide patterns displayed a transitional change through the seasons (Figure 3e).

The representative taxonomic groups were unique for each season (Figure 4), with only one taxon, *Alcaligenaceae*, identified as a core group among all seasons. The Aldex2 analysis revealed that there were no differentially expressed sOTUs between infected and uninfected frogs, but the relative abundance of three select microbes differed by season (Figure 4). Specifically, the microbial community composition in winter was significantly different than in all other seasons, and spring was different from fall. When comparing the winter to all other seasons, two sOTUs were differentially expressed (*Enterobacteriaceae*: $\text{Winter}_{CLR} = 10.743$, $\text{Other}_{CLR} = 1.753$; Effect Size = 2.526, $p > 0.001$; *Pseudomonas veronii*: $\text{Winter}_{CLR} = 11.771$, $\text{Other}_{CLR} = 1.200$; Effect Size = 2.863, $p > 0.001$). When comparing spring to fall, there was a single *Alcaligenaceae* sOTU differentially expressed ($\text{Spring}_{CLR} = 2.626$, $\text{Fall}_{CLR} = 9.946$; Effect Size = −1.744, $p > 0.001$).

3.5 | Individual-level correlations among mucosal attributes

Within individuals, stored peptide concentrations were negatively correlated with bacterial sOTU richness and predicted anti-*Bd* richness, but not correlated with the predicted anti-*Bd* function (Figure S1). Predicted anti-*Bd* function of the microbiome was consistently negatively related

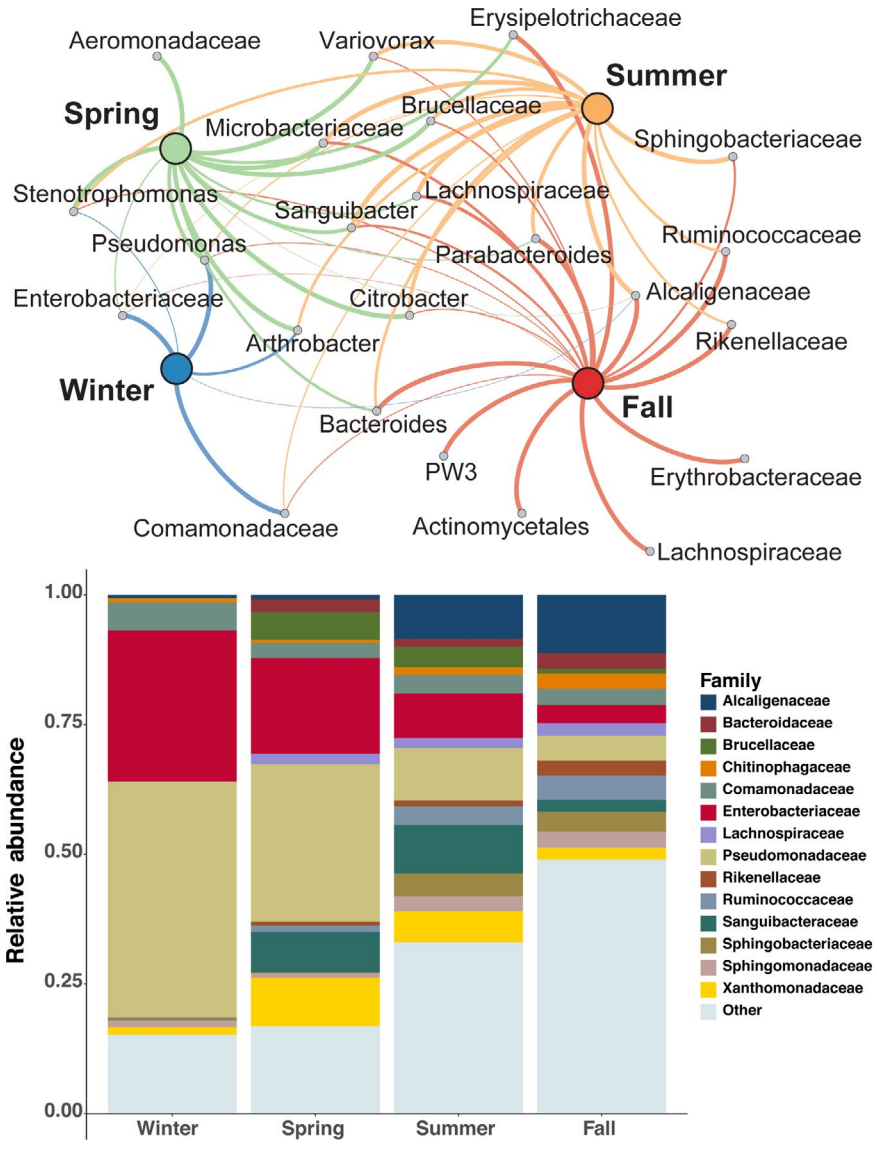

FIGURE 4 Top: Bipartite network showing the association of bacterial taxa from Southern leopard frog skin swabs by season (based on a 1% relative abundance threshold for sOTU inclusion). Lines connect family level sOTUs (shown by each smaller node) to each season (the four main nodes) and are weighted by relative abundance (sample sizes: winter = 17, spring = 13, summer = 30, fall = 24). Bottom: Taxonomic plot depicting relative abundance of the most abundant bacterial families by season

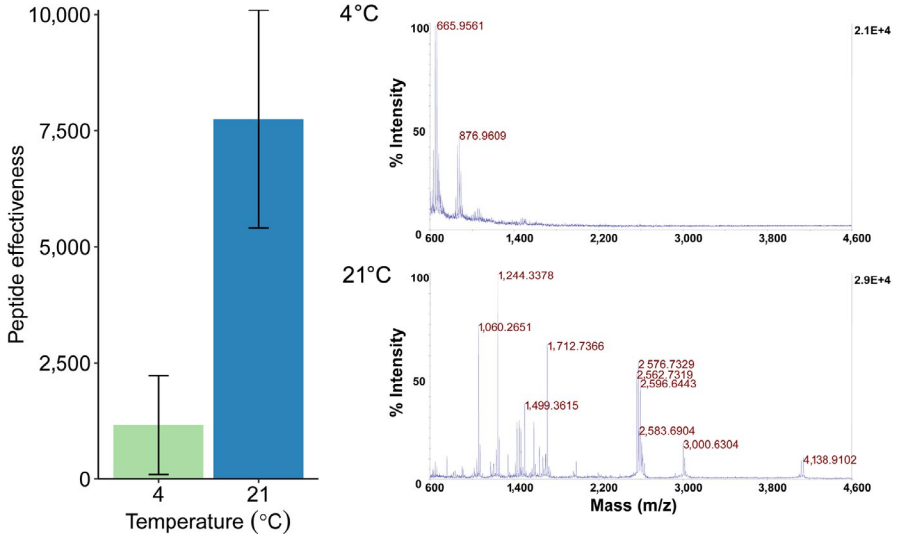

FIGURE 5 Left: After overwintering in the laboratory at 4°C, *Rana pipiens* adults recovered similar hydrophobic peptides, but they were less effective at inhibiting *Batrachochytrium dendrobatidis* (*Bd*) growth compared to those held at room temperature (21°C). Bars indicate average (±*SEM*) peptide effectiveness (product of recovered peptide concentration [μg/gbw] and inhibition of *Bd* growth at 50 μg/ml; $N = 4–6$). Right: Example MALDI-TOF spectra of recovered hydrophobic peptide secretions in frogs held at 4 and 21°C

to sOTU richness across seasons. However, when subsetting the microbiome dataset from this study to include only cultured sOTUs from the published database that have been tested for function (76.6 ± 23.6% of reads match the cultured bacteria, including those that facilitated or did not inhibit *Bd* growth), the same trends appear across seasons in anti-*Bd* function and anti-*Bd* sOTU richness. Thus, decreased anti-*Bd* function in the fall is not a reflection of changes in microbiome diversity obscuring the trend.

Of the nine recaptured animals, two had gained and two had lost infections and the rest remained uninfected, indicating that infection does not necessarily lead to chytridiomycosis or mortality. Microbiome diversity changes were large between captures, but typically peptide profiles were similar across recaptures even though time between captures varied from 12 to 176 days (Figure S2).

3.6 | Laboratory overwintered Northern leopard frogs

Secretions from frogs recovering at 4°C were less effective at inhibiting *Bd* growth compared to those held at 21°C (Mann–Whitney *U* test, $Z = -2.345$, $p = 0.019$; Figure 5). MALDI profiles have fewer peaks after cold treatment (Figure 5), although peptide concentrations were not significantly different (73.5 ± 49.4 μg/g compared to 103.5 ± 71.8 μg/g; Mann–Whitney *U*-test, $Z = -0.843$, $p = 0.476$). Specifically, peptide samples from six room temperature frogs ranged in activity from 58% to 100% *Bd* growth inhibition, whereas three of four cold-treated frogs had inhibition of *Bd* growth at <10%, indicating large differences in activity of secretions among groups.

4 | DISCUSSION

Seasonal disease dynamics are thought to be generated by annual host and pathogen biological rhythms interacting to affect epidemiological factors such as infection and transmission rates (Martinez-Bakker & Helm, 2015). Here, surveys of Southern leopard frogs revealed an annual cycle of greater *Bd* prevalence and loads during cooler months. Thus, we hypothesized that host immune cycles and pathogen growth cycles explain seasonal incidence of *Bd* in this host. Instead of pathogen growth (i.e. infection intensity) increasing when host defences were diminished, the peak of infection intensity and prevalence coincided with when frogs exhibited the greatest stored potential of AMPs and the highest predicted anti-*Bd* function of skin bacteria. Potentially accounting for times when cold temperatures slow AMP synthesis and most skin bacteria becoming dormant (Kueneman et al., 2019), frogs seemingly ramp up preparatory defences before winter. Perhaps Southern leopard frogs, which were never observed with signs of chytridiomycosis, may not need abundant storage of AMPs in the summer when temperature may greatly reduce *Bd* infections or boost other immune defences (reviewed in Rollins-Smith & Woodhams, 2012). Thus, the synchronicity in host–pathogen rhythms observed in this study appears to be weighted in the host's favour, with greater potential defences against *Bd* coinciding with higher risk of infection.

4.1 | Synchronicity of host–pathogen rhythms

Temperature and rainfall are known drivers of *Bd* dynamics (reviewed in Fisher et al., 2009); however, few studies quantify whether these factors also drive rhythms of host defences to influence seasonal patterns (except microbiome changes, discussed below). Here, host defence rhythms appear to play a role in seasonal *Bd* incidence, in that as temperatures warm in spring and more peptides are presumably released (stored concentrations decrease by ~2 fold from April to June), *Bd* loads and prevalence decrease. Then, after a period of diminished concentrations of stored AMPs and declining temperatures with the onset of fall, *Bd* incidence increases. Additional longitudinal data are needed to support this hypothesis; however, the decrease in stored peptide concentrations over spring can be interpreted as either greater secretion rates or similar secretion but slower synthesis rates. The latter seems unlikely given AMP recovery occurs

at a faster rate in warmer temperatures (discussed below). Thus, the spring trend of *Bd* infection can be explained by the combined actions of greater secretion of AMPs and warmer temperatures that increase clearance rates (Woodhams et al., 2003). The same mechanism can explain the trend in the fall: frogs accumulate greater stored peptide concentrations by reducing secretion rates, and temperature declines late fall start to increase *Bd* loads by stimulating pathogen growth and infectivity (Woodhams et al., 2008). This is could also explain the negative relationship between concentrations of stored peptides and *Bd* loads of frogs caught and sampled during winter. We interpret this as a reflection of greater secretion rates required to control infections during the cold season when synthesis of peptides is slower. However, longitudinal measures of peptide concentrations in the mucus and in storage are needed to confirm this hypothesis. Note that methods from this and referenced studies do not estimate constitutive concentrations in the skin mucus, or AMP synthesis and secretion rates which affect stored quantities. Only one previous study quantified stored AMP concentrations and *Bd* dynamics across seasons, and unlike this study, *Bd* peaked in the tropical frog *Colostethus panamensis* when stored anti-*Bd* AMP activity was low (Perez, 2015). Alternatively, Southern leopard frog mucosal defences and *Bd* rhythms could be coincidentally synchronized, both entrained to seasonal temperature cues, which was an important predictor of AMP concentrations and the probability of *Bd* infection.

4.2 | Seasonality of AMPs

Seasonal immunity is often associated with resource limitations or life-history trade-offs (reviewed in Martin et al., 2008). Considering that greater peptide storage coincided with periods of greater breeding activity (late fall or late winter), a trade-off between this aspect of immunity and reproductive effort seems unlikely. Although stored peptides increased following the season of higher resource availability (i.e. productivity in summer), body condition did not predict recovered peptide concentrations. Southern leopard frogs had greater stored peptide concentrations and more frequent expression of the full complement of AMPs during the cooler months, which contrasted most anurans studied previously. For instance, Matutte et al. (2000) found no AMP activity in *R. sylvatica* emerging from hibernation, but after a 3-week acclimation to 30°C, they expressed detectable AMP levels. Among species of *Litoria*, *L. rothii* did not express AMPs (i.e. caerins) in winter (Sherman et al., 2009), *L. splendida* and *L. citropa* had similar winter and summer AMP profiles (Wabnitz et al., 1999, 2000), and *L. peronii* expressed small concentrations in winter but not summer (Bilusich et al., 2009). As larvae, *L. serrata* (formerly *L. genimaculata*) expressed greater peptide concentrations with warmer stream temperatures (Rollins-Smith & Woodhams, 2012). In *Odorrana grahami*, seasonality of AMPs depended on population, with greater AMP activity during summer than fall in two populations, but another displayed the opposite pattern (Liu et al., 2018). Even a tropical species, *C. panamensis*, exhibited seasonality, with greater anti-*Bd* AMP activity during the dry compared to the wet season (Perez, 2015). Altogether, even closely related species may vary in seasonal AMP patterns and whether or not they coincide with elevated *Bd* risk. Thus, future work has the potential to identify whether these are endogenous rhythms and whether seasonal AMP expression is generalizable, because our understanding is based on relatively few species within only four anuran genera.

4.3 | Temperature-dependent AMP recovery

Greater storage of AMPs in winter and slower AMP recovery at lower temperatures support the hypothesis of a prophylactic response to the cold season (Ferguson et al., 2018), which has been shown in other innate immune responses in frogs (i.e. phagocyte activity; Marnila et al., 1995) and other vertebrates (e.g. lysozyme levels in Asian catfish; Kumari et al., 2006). Theoretically, temperature declines signal an adaptive shift to constitutive immune responses that are effective in the cold and to prepare for greater infection risk as temperatures warm in spring (Ferguson et al., 2018; Greenspan et al., 2017). In support of this hypothesis, extended exposure to cold temperatures reduced recovery of anti-*Bd* activity of secretions (this report), the relative intensity of AMPs in Southern leopard frogs (Robak et al., 2019), and peptide stores were ramped up before winter under natural conditions. Furthermore, AMP defences maintain inhibitory function even at low temperatures, whereas other immune defences may be slow to react (Cooper et al., 1992; Maniero & Carey, 1997). For instance, amphibian AMPs were just as effective in vitro at inactivating infectious ranaviruses at 4 and 26°C (Chinchar et al., 2004) and inhibiting *Bd* growth at both 10 and 22°C (Rollins-Smith, Carey, et al., 2002). Because skin bacteria can stimulate the release of specific AMPs (Mangoni et al., 2001), seasonal changes in diversity and abundance of skin microbes could play a role in preparing host AMP defences for winter.

4.4 | Seasonality of skin microbiome

Temporal shifts in diversity and structure of amphibian skin microbiomes appear common and have been related to *Bd* dynamics in several species (reviewed in Jiménez & Sommer, 2017). Most species display a reduction in diversity and relative richness during winter similar to this study (e.g. Tong et al., 2020), except *L. yavapaiensis* (Longo et al., 2015). Similar to *Rana catesbieana* gut microbiomes (Carr et al., 1976) the *Pseudomonadaceae* family dominated post-hibernation microbiomes in Southern leopard frogs. One of the differentially expressed sOTUs in this study, *Alcaligenaceae*, which increased in relative abundance during periods of low *Bd* prevalence, was previously shown to be more abundant proportionally to other groups on *Bd* negative frogs (Jimenez et al., 2019). Note that these proportional changes may not represent changes in bacterial biomass. The observation of greater abundance of bacterial dormancy genes in the microbiota of amphibian species

inhabiting more seasonal climates (Kueneman et al., 2019) suggests that the lower diversity in winter may be due to the majority of bacteria becoming dormant and then variable spring temperatures help diversify the microbiome. Moreover, host defences are known to regulate skin microbiomes (Holden, Reinert, et al., 2015; Küng et al., 2014). This mechanism is plausible given individual peptide concentrations were negatively correlated with alpha diversity, and the distance matrices of bacterial community and peptide profile were highly correlated, perhaps due to the addition of microbial metabolites or the selection of one aspect of skin defences on the other. Altogether, the microbiome of Southern leopard frogs appears more strongly affected by season than current *Bd* infection, similar to *L. yavapaiensis* (Longo et al., 2015). Perhaps similar to *R. sierrae* which experienced a loss of microbiome diversity when harbouring high *Bd* loads (Ellison et al., 2019; Jani & Briggs, 2014), previous *Bd* exposure may select for anti-*Bd* bacteria and lower microbial alpha diversity. Indeed, microbiome richness appears to reset over winter when antifungal bacteria become dominant, and then a steady recovery of bacterial residents increases diversity throughout the rest of the year when the potential *Bd* selection pressure lessens.

5 | CONCLUSIONS

These results demonstrate that seasonality of *Bd* in leopard frogs is dominated by annual temperature cycles, which is congruous with previous reports identifying the role of temperature regulating both host and pathogen processes (Robak et al., 2019; Woodhams et al., 2008). We interpret these results to suggest that mucosal defences are built up during the fall to accommodate potential insults to the skin during winter when cellular responses may be slow to react and infection risk is greatest. Because seasonal immunity corresponded to infection risk, comparative research has the potential to identify whether variation among species' tolerance to *Bd* can be explained by temporal rhythms in preparatory defences that coincide with the season of high infection risk. Given that *Bd*-associated population declines may have selected for more potent anti-*Bd* defences in recovering frog populations (in the absence of pathogen attenuation; Voyles et al., 2018), the potential for the observed immune rhythms to represent an evolutionary response warrants further research. Defining the mechanism underlying this preparatory response of investing in AMP storage—either an endogenous cycle or entrainment to environmental cues—is a critical gap for predicting climate change impacts. Our findings highlight the need for additional long-term and comparative surveys to identify how climate change-induced variation in seasonality may impact preparatory host defences and whether these defences may become temporally uncoupled from peaks in infection risk.

ACKNOWLEDGEMENTS

This research was supported by a Department of Defense Strategic Environmental Research and Development Program grant awarded to C.L.R.-Z. and sub-awarded to L.A.R.-S. and D.C.W. (RC-2638) and an NSF CAREER award to D.C.W. (IOS 1845634). We thank Bobby Fletcher, Brady Inman, Becky Hardman, Ann Sobell, Savannah Alford and Cody Engdahl for field survey assistance, Dan Wetzel for help with DNA extraction and qPCR, Joey Bonnaire for help with growth inhibition assays, and Molly Bletz for microbiome analysis advice. We also acknowledge the Mass Spectrometry Core Facilities at Vanderbilt University for MALDI-TOF instruments and analysis.

AUTHORS' CONTRIBUTIONS

C.L.R.-Z., L.A.R.-S. and D.C.W. designed and funded the research; L.A.R.-S., E.H.L.S., L.K.R. and B.T.M. collected data; E.H.L.S. and B.C.L. analysed data. All authors contributed to writing the manuscript.

DATA AVAILABILITY STATEMENT

Data are available on Dryad at https://doi.org/10.5061/dryad.ffbg79csh (Le Sage, 2020).

ORCID

Emily H. Le Sage https://orcid.org/0000-0002-2815-6651

REFERENCES

Altizer, S., Dobson, A., Hosseini, P., Hudson, P., Pascual, M., & Rohani, P. (2006). Seasonality and the dynamics of infectious diseases. *Ecology Letters*, *9*, 467–484. https://doi.org/10.1111/j.1461-0248.2005.00879.x

Altizer, S., Ostfeld, R. S., Johnson, P. T., Kutz, S., & Harvell, C. D. (2013). Climate change and infectious diseases: From evidence to a predictive framework. *Science*, *341*, 514–519. https://doi.org/10.1126/science.1239401

Amir, A., McDonald, D., Navas-Molina, J. A., Kopylova, E., Morton, J. T., Zech Xu, Z., Kightley, E. P., Thompson, L. R., Hyde, E. R., Gonzalez, A., & Knight, R. (2017). Deblur rapidly resolves single-nucleotide community sequence patterns. *mSystems*, *2*(2). https://doi.org/10.1128/mSystems.00191-16

Antwis, R. E., & Harrison, X. A. (2018). Probiotic consortia are not uniformly effective against different amphibian chytrid pathogen isolates. *Molecular Ecology*, *27*, 577–589. https://doi.org/10.1111/mec.14456

Bastian, M., Heymann, S., & Jacomy, M. (2009). Gephi: An open source software for exploring and manipulating networks. In *Third International ICWSM Conference*, pp. 361–362.

Berger, L., Speare, R., Hines, H. B., Marantelli, G., Hyatt, A. D., McDONALD, K. R., Skerratt, L. F., Olsen, V., Clarke, J. M., Gillespie, G., Mahony, M., Sheppard, N., Williams, C., & Tyler, M. J. (2004). Effect of season and temperature on mortality in amphibians due to chytridiomycosis. *Australian Veterinary Journal*, *82*, 434–439. https://doi.org/10.1111/j.1751-0813.2004.tb11137.x

Bilusich, D., Jackway, R. J., Musgrave, I. F., Tyler, M. J., & Bowie, J. H. (2009). The host-defence skin peptide profiles of Peron's Tree Frog *Litoria peronii* in winter and summer. Sequence determination by electrospray mass spectrometry and activities of the peptides. *Rapid Communications in Mass Spectrometry: An International Journal Devoted to the Rapid Dissemination of Up-to-the-Minute Research in Mass Spectrometry*, *23*, 2628–2636.

Bletz, M. C., Loudon, A. H., Becker, M. H., Bell, S. C., Woodhams, D. C., Minbiole, K. P., & Harris, R. N. (2013). Mitigating amphibian chytridiomycosis with bioaugmentation: Characteristics of effective

probiotics and strategies for their selection and use. *Ecology Letters*, *16*, 807–820. https://doi.org/10.1111/ele.12099

Blooi, M., Pasmans, F., Longcore, J. E., Spitzen-Van Der Sluijs, A., Vercammen, F., & Martel, A. (2013). Duplex real-time PCR for rapid simultaneous detection of *Batrachochytrium dendrobatidis* and *Batrachochytrium salamandrivorans* in amphibian samples. *Journal of Clinical Microbiology*, *51*, 4173–4177. https://doi.org/10.1128/JCM.02313-13

Bolyen, E., Rideout, J. R., Dillon, M. R., Bokulich, N. A., Abnet, C. C., Al-Ghalith, G. A., Alexander, H., Alm, E. J., Arumugam, M., Asnicar, F., Bai, Y., Bisanz, J. E., Bittinger, K., Brejnrod, A., Brislawn, C. J., Brown, C. T., Callahan, B. J., Caraballo-Rodríguez, A. M., Chase, J., … Caporaso, J. G. (2019). Reproducible, interactive, scalable and extensible microbiome data science using QIIME 2. *Nature Biotechnology*, *37*(8), 852–857. https://doi.org/10.1038/s41587-019-0209-9

Caporaso, J. G., Lauber, C. L., Walters, W. A., Berg-Lyons, D., Huntley, J., Fierer, N., Owens, S. M., Betley, J., Fraser, L., Bauer, M., Gormley, N., Gilbert, J. A., Smith, G., & Knight, R. (2012). Ultra-high-throughput microbial community analysis on the Illumina HiSeq and MiSeq platforms. *The ISME Journal*, *6*, 1621–1624. https://doi.org/10.1038/ismej.2012.8

Carr, A. H., Amborski, R. L., Culley, D. D. Jr, & Amborski, G. F. (1976). Aerobic bacteria in the intestinal tracts of bullfrogs (*Rana catesbeiana*) maintained at low temperatures. *Herpetologica*, 239–244.

Chinchar, V., Bryan, L., Silphadaung, U., Noga, E., Wade, D., & Rollins-Smith, L. (2004). Inactivation of viruses infecting ectothermic animals by amphibian and piscine antimicrobial peptides. *Virology*, *323*, 268–275. https://doi.org/10.1016/j.virol.2004.02.029

Conlon, T. J., Halverson, T., Dulka, J., Platz, J., & Knoop, F. (1999). Peptides with antimicrobial activity of the brevinin-1 family isolated from skin secretions of the southern leopard frog, *Rana sphenocephala*. *Chemical Biology & Drug Design*, *54*, 522–527.

Cooper, E. L., Wright, R. K., Klempau, A. E., & Smith, C. T. (1992). Hibernation alters the frog's immune system. *Cryobiology*, *29*, 616–631. https://doi.org/10.1016/0011-2240(92)90066-B

Davenport, E. R., Mizrahi-Man, O., Michelini, K., Barreiro, L. B., Ober, C., & Gilad, Y. (2014). Seasonal variation in human gut microbiome composition. *PLoS ONE*, *9*, e90731. https://doi.org/10.1371/journal.pone.0090731

Dopico, X. C., Evangelou, M., Ferreira, R. C., Guo, H., Pekalski, M. L., Smyth, D. J., Cooper, N., Burren, O. S., Fulford, A. J., Hennig, B. J., Prentice, A. M., Ziegler, A.-G., Bonifacio, E., Wallace, C., & Todd, J. A. (2015). Widespread seasonal gene expression reveals annual differences in human immunity and physiology. *Nature Communications*, *6*, 1–13. https://doi.org/10.1038/ncomms8000

Ellison, S., Knapp, R. A., Sparagon, W., Swei, A., & Vredenburg, V. T. (2019). Reduced skin bacterial diversity correlates with increased pathogen infection intensity in an endangered amphibian host. *Molecular Ecology*, *28*, 127–140. https://doi.org/10.1111/mec.14964

Estrada, A., Hughey, M. C., Medina, D., Rebollar, E. A., Walke, J. B., Harris, R. N., & Belden, L. K. (2019). Skin bacterial communities of neotropical treefrogs vary with local environmental conditions at the time of sampling. *PeerJ*, *7*, e7044. https://doi.org/10.7717/peerj.7044

Ferguson, L. V., Kortet, R., & Sinclair, B. J. (2018). Eco-immunology in the cold: The role of immunity in shaping the overwintering survival of ectotherms. *Journal of Experimental Biology*, *221*, jeb163873. https://doi.org/10.1242/jeb.163873

Fernandes, A. D., Reid, J. N., Macklaim, J. M., McMurrough, T. A., Edgell, D. R., & Gloor, G. B. (2014). Unifying the analysis of high-throughput sequencing datasets: Characterizing RNA-seq, 16S rRNA gene sequencing and selective growth experiments by compositional data analysis. *Microbiome*, *2*, 15. https://doi.org/10.1186/2049-2618-2-15

Fisher, M. C., Garner, T. W., & Walker, S. F. (2009). Global emergence of *Batrachochytrium dendrobatidis* and amphibian chytridiomycosis in space, time, and host. *Annual Review of Microbiology*, *63*, 291–310.

Garland, S., Baker, A., Phillott, A. D., & Skerratt, L. F. (2010). BSA reduces inhibition in a TaqMan® assay for the detection of *Batrachochytrium dendrobatidis*. *Diseases of Aquatic Organisms*, *92*, 113–116. https://doi.org/10.3354/dao02053

Goelen, T., Sobhy, I. S., Vanderaa, C., Wäckers, F., Rediers, H., Wenseleers, T., Jacquemyn, H., & Lievens, B. (2020). Bacterial phylogeny predicts volatile organic compound composition and olfactory response of an aphid parasitoid. *Oikos*, *129*(9), 1415–1428. https://doi.org/10.1111/oik.07301

Grassly, N. C., & Fraser, C. (2006). Seasonal infectious disease epidemiology. *Proceedings of the Royal Society B: Biological Sciences*, *273*, 2541–2550. https://doi.org/10.1098/rspb.2006.3604

Gray, M., Duffus, A., Haman, K., Harris, R., Allender, M., Thompson, T., Christman, M., Sacerdote-Velat, A., Sprague, L., & Williams, J. (2017). Pathogen surveillance in herpetofaunal populations: Guidance on study design, sample collection, biosecurity, and intervention strategies. *Herpetological Review*, *48*, 334–351.

Greenspan, S. E., Bower, D. S., Webb, R. J., Berger, L., Rudd, D., Schwarzkopf, L., & Alford, R. A. (2017). White blood cell profiles in amphibians help to explain disease susceptibility following temperature shifts. *Developmental & Comparative Immunology*, *77*, 280–286. https://doi.org/10.1016/j.dci.2017.08.018

Hall, E. M., Goldberg, C., Brunner, J., & Crespi, E. (2018). Seasonal dynamics and potential drivers of ranavirus epidemics in wood frog populations. *Oecologia*, *188*, 1253–1262. https://doi.org/10.1007/s00442-018-4274-4

Harvell, C. D., Mitchell, C. E., Ward, J. R., Altizer, S., Dobson, A. P., Ostfeld, R. S., & Samuel, M. D. (2002). Climate warming and disease risks for terrestrial and marine biota. *Science*, *296*, 2158. https://doi.org/10.1126/science.1063699

Holden, W. M., Hanlon, S. M., Woodhams, D. C., Chappell, T. M., Wells, H. L., Glisson, S. M., McKenzie, V. J., Knight, R., Parris, M. J., & Rollins-Smith, L. A. (2015). Skin bacteria provide early protection for newly metamorphosed southern leopard frogs (*Rana sphenocephala*) against the frog-killing fungus, *Batrachochytrium dendrobatidis*. *Biological Conservation*, *187*, 91–102. https://doi.org/10.1016/j.biocon.2015.04.007

Holden, W. M., Reinert, L. K., Hanlon, S. M., Parris, M. J., & Rollins-Smith, L. A. (2015). Development of antimicrobial peptide defenses of southern leopard frogs, *Rana sphenocephala*, against the pathogenic chytrid fungus, *Batrachochytrium dendrobatidis*. *Developmental & Comparative Immunology*, *48*, 65–75. https://doi.org/10.1016/j.dci.2014.09.003

Hyatt, A. D., Boyle, D. G., Olsen, V., Boyle, D. B., Berger, L., Obendorf, D., Dalton, A., Kriger, K., Hero, M., Hines, H., Phillott, R., Campbell, R., Marantelli, G., Gleason, F., & Colling, A. (2007). Diagnostic assays and sampling protocols for the detection of *Batrachochytrium dendrobatidis*. *Diseases of Aquatic Organisms*, *73*, 175–192. https://doi.org/10.3354/dao073175

Jani, A. J., & Briggs, C. J. (2014). The pathogen *Batrachochytrium dendrobatidis* disturbs the frog skin microbiome during a natural epidemic and experimental infection. *Proceedings of the National Academy of Sciences of the United States of America*, *111*, E5049–E5058.

Jenkins, E., Veitch, A., Kutz, S., Hoberg, E., & Polley, L. (2006). Climate change and the epidemiology of protostrongylid nematodes in northern ecosystems: *Parelaphostrongylus odocoilei* and *Protostrongylus stilesi* in Dall's sheep (*Ovis d. dalli*). *Parasitology*, *132*, 387–401.

Jimenez, R. R., Alvarado, G., Estrella, J., & Sommer, S. (2019). Moving beyond the host: Unraveling the skin microbiome of endangered costa Rican amphibians. *Frontiers in Microbiology*, *10*, 2060. https://doi.org/10.3389/fmicb.2019.02060

Jiménez, R. R., & Sommer, S. (2017). The amphibian microbiome: Natural range of variation, pathogenic dysbiosis, and role in conservation. *Biodiversity and Conservation*, *26*, 763–786. https://doi.org/10.1007/s10531-016-1272-x

Kriger, K. M., Hero, J.-M., & Ashton, K. J. (2006). Cost efficiency in the detection of chytridiomycosis using PCR assay. *Diseases of Aquatic Organisms*, *71*, 149–154. https://doi.org/10.3354/dao071149

Kueneman, J. G., Bletz, M. C., McKenzie, V. J., Becker, C. G., Joseph, M. B., Abarca, J. G., Archer, H., Arellano, A. L., Bataille, A., Becker, M., Belden, L. K., Crottini, A., Geffers, R., Haddad, C. F. B., Harris, R. N., Holden, W. M., Hughey, M., Jarek, M., Kearns, P. J., … Vences, M. (2019). Community richness of amphibian skin bacteria correlates with bioclimate at the global scale. *Nature Ecology & Evolution*, *3*, 381–389. https://doi.org/10.1038/s41559-019-0798-1

Kumari, J., Sahoo, P., Swain, T., Sahoo, S., Sahu, A., & Mohanty, B. (2006). Seasonal variation in the innate immune parameters of the Asian catfish *Clarias batrachus*. *Aquaculture*, *252*, 121–127. https://doi.org/10.1016/j.aquaculture.2005.07.025

Küng, D., Bigler, L., Davis, L. R., Gratwicke, B., Griffith, E., & Woodhams, D. C. (2014). Stability of microbiota facilitated by host immune regulation: Informing probiotic strategies to manage amphibian disease. *PLoS ONE*, *9*. https://doi.org/10.1371/journal.pone.0087101

Kuznetsova, A., Brockhoff, P. B., & Christensen, R. H. B. (2017). lmerTest package: Tests in linear mixed effects models. *Journal of Statistical Software*, *82*, 1–26.

Langille, M. G. I., Zaneveld, J., Caporaso, J. G., McDonald, D., Knights, D., Reyes, J. A., Clemente, J. C., Burkepile, D. E., Vega Thurber, R. L., Knight, R., Beiko, R. G., & Huttenhower, C. (2013). Predictive functional profiling of microbial communities using 16S rRNA marker gene sequences. *Nature Biotechnology*, *31*, 814–821. https://doi.org/10.1038/nbt.2676

Le Sage, E. (2020). Data from: Preparatory immunity: Seasonality of mucosal skin defenses and *Batrachochytrium* infections in Southern leopard frogs [Dataset]. *Dryad*, https://doi.org/10.5061/dryad.ffbg79csh

Liu, J., Chen, Z., Chen, G., Wang, B., & Jiang, J. (2018). Skin innate immunity of diskless-fingered odorous frogs (*Odorrana grahami*) with spatial-temporal variations. *Developmental & Comparative Immunology*, *89*, 23–30. https://doi.org/10.1016/j.dci.2018.08.003

Longo, A. V., Savage, A. E., Hewson, I., & Zamudio, K. R. (2015). Seasonal and ontogenetic variation of skin microbial communities and relationships to natural disease dynamics in declining amphibians. *Royal Society Open Science*, *2*, 140377. https://doi.org/10.1098/rsos.140377

Mangoni, M. L., Miele, R., Renda, T. G., Barra, D., & Simmaco, M. (2001). The synthesis of antimicrobial peptides in the skin of *Rana esculenta* is stimulated by microorganisms. *The FASEB Journal*, *15*, 1431–1432.

Maniero, G. D., & Carey, C. (1997). Changes in selected aspects of immune function in the leopard frog, *Rana pipiens*, associated with exposure to cold. *Journal of Comparative Physiology B: Biochemical, Systemic, and Environmental Physiology*, *167*, 256–263. https://doi.org/10.1007/s003600050072

Marnila, P., Tiiska, A., Lagerspetz, K., & Lilius, E.-M. (1995). Phagocyte activity in the frog *Rana temporaria*: Whole blood chemiluminescence method and the effects of temperature and thermal acclimation. *Comparative Biochemistry and Physiology Part A: Physiology*, *111*, 609–614. https://doi.org/10.1016/0300-9629(95)00054-B

Martin, L. B., Weil, Z. M., & Nelson, R. J. (2008). Seasonal changes in vertebrate immune activity: Mediation by physiological trade-offs. *Philosophical Transactions of the Royal Society B: Biological Sciences*, *363*, 321–339. https://doi.org/10.1098/rstb.2007.2142

Martinez-Bakker, M., & Helm, B. (2015). The influence of biological rhythms on host-parasite interactions. *Trends in Ecology & Evolution*, *30*, 314–326. https://doi.org/10.1016/j.tree.2015.03.012

Matutte, B., Storey, K. B., Knoop, F. C., & Conlon, J. M. (2000). Induction of synthesis of an antimicrobial peptide in the skin of the freeze-tolerant frog, *Rana sylvatica*, in response to environmental stimuli. *FEBS Letters*, *483*, 135–138.

McDonald, D., Price, M. N., Goodrich, J., Nawrocki, E. P., DeSantis, T. Z., Probst, A., Andersen, G. L., Knight, R., & Hugenholtz, P. (2012). An improved Greengenes taxonomy with explicit ranks for ecological and evolutionary analyses of bacteria and archaea. *The ISME Journal*, *6*, 610. https://doi.org/10.1038/ismej.2011.139

Nelson, R. J., & Demas, G. E. (1996). Seasonal changes in immune function. *Quarterly Review of Biology*, 511–548. https://doi.org/10.1086/419555

Oksanen, J., Blanchet, F. G., Friendly, M., Kindt, R., Legendre, P., McGlinn, D., Minchin, P. R., O'Hara, R. B., Simpson, G. L., Solymos, P., Stevens, M. H. H., Szoecs, E., & Wagner, H. (2019). *vegan: Community Ecology Package*. R package version 2.5-6. Retrieved from https://CRAN.R-project.org/package=vegan

Pask, J. D., Woodhams, D. C., & Rollins-Smith, L. A. (2012). The ebb and flow of antimicrobial skin peptides defends Northern leopard frogs (*Rana pipiens*) against chytridiomycosis. *Global Change Biology*, *18*, 1231–1238. https://doi.org/10.1111/j.1365-2486.2011.02622.x

Perez, R. G. (2015). *A closer look: Seasonality patterns of skin peptides and microhabitat temperatures in surviving* Colostethus panamensis *after disease outbreak in Panama*. New Mexico Institute of Mining and Technology.

Raffel, T., Rohr, J., Kiesecker, J., & Hudson, P. (2006). Negative effects of changing temperature on amphibian immunity under field conditions. *Functional Ecology*, *20*, 819–828. https://doi.org/10.1111/j.1365-2435.2006.01159.x

Ramsey, J. P., Reinert, L. K., Harper, L. K., Woodhams, D. C., & Rollins-Smith, L. A. (2010). Immune defenses against *Batrachochytrium dendrobatidis*, a fungus linked to global amphibian declines, in the South African clawed frog, *Xenopus laevis*. *Infection and Immunity*, *78*, 3981–3992. https://doi.org/10.1128/IAI.00402-10

Robak, M. J., Reinert, L. K., Rollins-Smith, L. A., & Richards-Zawacki, C. L. (2019). Out in the cold and sick: Low temperatures and fungal infections impair a frog's skin defenses. *Journal of Experimental Biology*, *222*, jeb209445. https://doi.org/10.1242/jeb.209445

Rognes, T., Flouri, T., Nichols, B., Quince, C., & Mahé, F. (2016). VSEARCH: A versatile open source tool for metagenomics. *PeerJ*, *4*, e2584. https://doi.org/10.7717/peerj.2584

Rollins-Smith, L. (2020). Global amphibian declines, disease, and the ongoing battle between *Batrachochytrium* fungi and the immune system. *Herpetologica*, *76*, 178. https://doi.org/10.1655/0018-0831-76.2.178

Rollins-Smith, L. A., Carey, C., Longcore, J., Doersam, J. K., Boutte, A., Bruzgal, J. E., & Conlon, J. M. (2002). Activity of antimicrobial skin peptides from ranid frogs against *Batrachochytrium dendrobatidis*, the chytrid fungus associated with global amphibian declines. *Developmental & Comparative Immunology*, *26*, 471–479. https://doi.org/10.1016/S0145-305X(01)00088-X

Rollins-Smith, L. A., Doersam, J. K., Longcore, J. E., Taylor, S. K., Shamblin, J. C., Carey, C., & Zasloff, M. A. (2002). Antimicrobial peptide defenses against pathogens associated with global amphibian declines. *Developmental & Comparative Immunology*, *26*, 63–72. https://doi.org/10.1016/S0145-305X(01)00041-6

Rollins-Smith, L. A., & Woodhams, D. C. (2012). *Amphibian immunity*. Oxford University Press.

Runckel, C., Flenniken, M. L., Engel, J. C., Ruby, J. G., Ganem, D., Andino, R., & DeRisi, J. L. (2011). Temporal analysis of the honey bee microbiome reveals four novel viruses and seasonal prevalence of known viruses, Nosema, and Crithidia. *PLoS ONE*, *6*, e20656. https://doi.org/10.1371/journal.pone.0020656

Sandmeier, F., Horn, K., & Tracy, C. (2016). Temperature-independent, seasonal fluctuations in immune function of the Mojave Desert Tortoise (*Gopherus agassizii*). *Canadian Journal of Zoology*, *94*, 583–590.

Sedlar, K., Videnska, P., Skutkova, H., Rychlik, I., & Provaznik, I. (2016). Bipartite graphs for visualization analysis of microbiome data: Supplementary issue: Bioinformatics methods and applications for big metagenomics data. *Evolutionary Bioinformatics*, *12*, EBO.S38546. https://doi.org/10.4137/EBO.S38546

Shaman, J., Pitzer, V. E., Viboud, C., Grenfell, B. T., & Lipsitch, M. (2010). Absolute humidity and the seasonal onset of influenza in the continental United States. *PLoS Biology*, *8*, e1000316.

Sheldon, B. C., & Verhulst, S. (1996). Ecological immunology: Costly parasite defences and trade-offs in evolutionary ecology. *Trends in Ecology & Evolution*, *11*, 317–321. https://doi.org/10.1016/0169-5347(96)10039-2

Sherman, P. J., Jackway, R. J., Nicholson, E., Musgrave, I. F., Boontheung, P., & Bowie, J. H. (2009). Activities of seasonably variable caerulein and rothein skin peptides from the tree frogs *Litoria splendida* and *Litoria rothii*. *Toxicon*, *54*, 828–835. https://doi.org/10.1016/j.toxicon.2009.06.009

Stevenson, T. J., Visser, M. E., Arnold, W., Barrett, P., Biello, S., Dawson, A., Denlinger, D. L., Dominoni, D., Ebling, F. J., Elton, S., Evans, N., Ferguson, H. M., Foster, R. G., Hau, M., Haydon, D. T., Hazlerigg, D. G., Heideman, P., Hopcraft, J. G. C., Jonsson, N. N., … Helm, B. (2015). Disrupted seasonal biology impacts health, food security and ecosystems. *Proceedings of the Royal Society B: Biological Sciences*, *282*, 20151453. https://doi.org/10.1098/rspb.2015.1453

Szwejser, E., Verburg-van Kemenade, B. L., Maciuszek, M., & Chadzinska, M. (2017). Estrogen-dependent seasonal adaptations in the immune response of fish. *Hormones and Behavior*, *88*, 15–24. https://doi.org/10.1016/j.yhbeh.2016.10.007

Tong, Q., Hu, Z.-F., Du, X.-P., Bie, J., & Wang, H.-B. (2020). Effects of seasonal hibernation on the similarities between the skin microbiota and gut microbiota of an amphibian (*Rana dybowskii*). *Environmental Microbiology*, *79*, 898–909. https://doi.org/10.1007/s00248-019-01466-9

Visser, M. E., Caro, S. P., Van Oers, K., Schaper, S. V., & Helm, B. (2010). Phenology, seasonal timing and circannual rhythms: Towards a unified framework. *Philosophical Transactions of the Royal Society B: Biological Sciences*, *365*, 3113–3127.

Voyles, J., Woodhams, D. C., Saenz, V., Byrne, A. Q., Perez, R., Rios-Sotelo, G., Ryan, M. J., Bletz, M. C., Sobell, F. A., McLetchie, S., Reinert, L., Rosenblum, E. B., Rollins-Smith, L. A., Ibáñez, R., Ray, J. M., Griffith, E. J., Ross, H., & Richards-Zawacki, C. L. (2018). Shifts in disease dynamics in a tropical amphibian assemblage are not due to pathogen attenuation. *Science*, *359*, 1517. https://doi.org/10.1126/science.aao4806

Wabnitz, P. A., Bowie, J. H., & Tyler, M. J. (1999). Caerulein-like peptides from the skin glands of the Australian Blue Mountains tree frog *Litoria citropa*. Part 1. Sequence determination using electrospray mass spectrometry. *Rapid Communications in Mass Spectrometry*, *13*, 2498–2502. https://doi.org/10.1002/(SICI)1097-0231(19991230)13:24<2498:AID-RCM817>3.0.CO;2-E

Wabnitz, P. A., Bowie, J. H., Tyler, M. J., Wallace, J. C., & Smith, B. P. (2000). Differences in the skin peptides of the male and female Australian tree frog *Litoria splendida*: The discovery of the aquatic male sex pheromone splendipherin, together with Phe8 caerulein and a new antibiotic peptide caerin 1.10. *European Journal of Biochemistry*, *267*, 269–275. https://doi.org/10.1046/j.1432-1327.2000.01010.x

Williams, C. M., Henry, H. A. L., & Sinclair, B. J. (2015). Cold truths: How winter drives responses of terrestrial organisms to climate change. *Biological Reviews*, *90*, 214–235. https://doi.org/10.1111/brv.12105

Woodhams, D. C., Alford, R. A., Antwis, R. E., Archer, H., Becker, M. H., Belden, L. K., Bell, S. C., Bletz, M., Daskin, J. H., Davis, L. R., Flechas, S. V., Lauer, A., Gonzalez, A., Harris, R. N., Holden, W. M., Hughey, M. C., Ibáñez, R., Knight, R., Kueneman, J., … McKenzie, V. (2015). Antifungal isolates database of amphibian skin-associated bacteria and function against emerging fungal pathogens: Ecological Archives E096–059. *Ecology*, *96*, 595. https://doi.org/10.1890/14-1837.1

Woodhams, D. C., Alford, R. A., Briggs, C. J., Johnson, M., & Rollins-Smith, L. A. (2008). Life-history trade-offs influence disease in changing climates: Strategies of an amphibian pathogen. *Ecology*, *89*, 1627–1639. https://doi.org/10.1890/06-1842.1

Woodhams, D. C., Alford, R. A., & Marantelli, G. (2003). Emerging disease of amphibians cured by elevated body temperature. *Diseases of Aquatic Organisms*, *55*, 65–67. https://doi.org/10.3354/dao055065

Woodhams, D. C., Brandt, H., Baumgartner, S., Kielgast, J., Kupfer, E., Tobler, U., Davis, L. R., Schmidt, B. R., Bel, C., Hodel, S., Knight, R., & McKenzie, V. (2014). Interacting symbionts and immunity in the amphibian skin mucosome predict disease risk and probiotic effectiveness. *PLoS ONE*, *9*, e96375. https://doi.org/10.1371/journal.pone.0096375

SUPPORTING INFORMATION

Additional supporting information may be found online in the Supporting Information section.

How to cite this article: Le Sage EH, LaBumbard BC, Reinert LK, et al. Preparatory immunity: Seasonality of mucosal skin defences and *Batrachochytrium* infections in Southern leopard frogs. *J Anim Ecol*. 2020;00:1–14. https://doi.org/10.1111/1365-2656.13386